



Article

Static and Dynamic Mechanical Behavior of Carbon Fiber Reinforced Plastic (CFRP) Single-Lap Shear Joints Joule-Bonded with Conductive Epoxy Nanocomposites

Yuheng Huang, Ian A. Kinloch and Cristina Vallés *

Department of Materials, National Graphene Institute and Henry Royce Institute, University of Manchester, Oxford Road, Manchester M13 9PL, UK; yuheng.huang-2@postgrad.manchester.ac.uk (Y.H.); ian.kinloch@manchester.ac.uk (I.A.K.)

* Correspondence: cristina.valles@manchester.ac.uk

Abstract: The potential of electrically conductive graphene nanoplatelets (GNPs)/epoxy, multi-walled carbon nanotubes (MWCNTs)/epoxy and hybrid GNPs-MWCNTs/epoxy nanocomposites as adhesives for out-of-autoclave (OoA) and in-the-field CFRP repair via Joule heat curing was investigated. Scanning electron microscopy revealed a good dispersion of the nanoparticles in the matrix in all the nanocomposite adhesives above their percolation thresholds, which led to a homogeneous distribution of the heat generated during Joule CFRP repair. The joints bonded with neat epoxy and the nanocomposites showed similar lap shear strengths, with the addition of nanoparticles enhancing the fatigue performance of the adhesively bonded joints relative to when neat epoxy was used as an adhesive and oven-cured. The interfacial and cohesive failure mechanisms were found to coexist in all the cases, with an increasing dominance of the cohesive when nanofillers were embedded into the adhesive. No effect of the specific type of nanofiller incorporated into the epoxy as the conductive component was observed on the mechanical performance of the bonded joints, with the adhesives containing MWCNTs showing similar results to those filled with GNPs at considerably lower loadings due to their lower percolation thresholds. The independence of the properties regardless of the curing method highlights the promise of these Joule-cured adhesives for industrial applications.

Keywords: graphene; carbon nanotubes; epoxy nanocomposites; adhesive joints; lap shear strength; fatigue resistance



Citation: Huang, Y.; Kinloch, I.A.; Vallés, C. Static and Dynamic Mechanical Behavior of Carbon Fiber Reinforced Plastic (CFRP) Single-Lap Shear Joints Joule-Bonded with Conductive Epoxy Nanocomposites. *J. Compos. Sci.* **2024**, *8*, 112. <https://doi.org/10.3390/jcs8030112>

Academic Editors: Xiangfa Wu and Oksana Zholobko

Received: 18 January 2024

Revised: 6 March 2024

Accepted: 12 March 2024

Published: 21 March 2024



Copyright: © 2024 by the authors. Licensee MDPI, Basel, Switzerland. This article is an open access article distributed under the terms and conditions of the Creative Commons Attribution (CC BY) license (<https://creativecommons.org/licenses/by/4.0/>).

1. Introduction

Carbon fiber-reinforced plastics (CFRPs) are increasingly used in many industrial sectors due to their high specific strength and stiffness, low density, multifunctionality, easy integration into consolidated components and design versatility. In particular, driven by new targets for lower CO₂ emissions and the need for light-weight structures, the global demand for these composites in the aerospace, construction, wind energy and automotive sectors is expected to continue to grow [1,2]. In 2000, specific goals for delivering significant improvements in sustainable, reliable, affordable and passenger-friendly aviation were a 50% cut in CO₂ emissions per passenger per km (i.e., 50% cut in fuel consumption in the new aircrafts of 2020) and an 80% cut in NO emissions, with the current initiative targeting net zero CO₂ emissions by 2050 [3]. The use of CFRPs contributes enormously to a reduction in the overall weight of the aircraft's structure, thus leading to important reductions in fuel consumption, and hence, in CO₂ and NO emissions. In general terms, 3.1 kg of CO₂ is generated for every kg of fuel used; thus, the reduction of one kg built-in aircraft weight can reduce carbon emissions by 0.94 kg in the case of the Boeing 747–400, whose weight is 396,890 kg, and by 0.475 kg in the Airbus A330-300, whose weight is 242,000 kg [4]. This rapid growth in the adoption of CFRPs is, however, leading to major environmental

challenges in waste management, which includes off-cuts generated during composite manufacturing and end-of-life CFRP products [5–7]. Thus, there is currently an urgent demand for the development of efficient and sustainable techniques for CFRP repair.

Polymeric adhesives have been widely used in the past to join CFRPs, because they offer important advantages compared to more traditional methods of joining CFRPs such as bolting, brazing, welding, mechanical fasteners, etc. [8]. Such advantages include the ability to join dissimilar materials to give light-weight but strong and stiff structures, and to efficiently join thin-sheet materials, which, due to their low bearing strength, cannot be joined by other methods. In addition, adhesive bonding represents the most flexible and convenient method for joining materials with versatile design options and also offering an easy automation [9]. For these reasons, adhesive bonding is widely used in many industries, including in the automobile, truck, aerospace, railway and electronic industries [10], with epoxy adhesives, in particular, representing the most common type of structural adhesive. When polymerized, epoxy adhesives acquire a highly crosslinked microstructure, which results in many useful properties for structural engineering applications, such as a high modulus and failure strength, low creep and good performance at elevated temperatures [11,12]. However, in most of the cases, heat needs to be applied to promote the crosslinking reaction and facilitate the formation of covalent bonds, with such heat curing processes being typically performed in an autoclave, which use is labor-intensive and involves both high energy consumption and a high cost [13]. In addition, autoclave curing or repair also involves having to heat the whole component, which can lead to unwanted structural changes. Thus, OoA strategies to cure composite repairs locally on damaged structures outside an oven or autoclave, providing highly localized heating that avoids heating the whole component, while also avoiding the large time and energy consumption typically associated with the use of an oven/autoclave, are currently required.

The incorporation of electrically conductive nanofillers into the epoxy adhesives emerges as a good alternative to the use of an oven or autoclave for CFRP repair through adhesively bonded joints. Electrically conductive materials and, more specifically, carbon nanomaterials have been recently proved to effectively transform an electric current into heat through a simple Joule heating effect of the electrically conductive network of carbon nanoparticles embedded in a polymer matrix above their percolation threshold [14]. Some research has been reported on the application of such electrothermal property to de-icing systems [15], as well as to the development of novel OoA thermosets curing methods. For example, Mas et al. reported the curing of epoxy resins through Joule heating of carbon nanotubes (CNTs) and graphene embedded in the polymer above the electrical percolation threshold [16], where the small distance between the nanocarbon particles (<100 nm) was found to render a fast heating rate and a better distribution of the heat relative to the oven-based cure. The potential of this resistive heating in applications such as aerospace composite parts repair, glass fiber composite laminate fabrication, and soldering of an assembly of CNTs to a metal substrate was also explored in that work. Other researchers have studied the effect of the nature and amount of different carbon nanofillers (CNTs vs. graphene) on the self-heating of epoxy composites, finding that the composites filled with CNTs reach higher temperatures than those reinforced with graphene nanoplatelets (GNPs) applying lower electrical voltage because of their higher electrical conductivities, with the self-heating being, however, more homogeneous for the GNP/epoxy resins due to their higher thermal conductivity [17]. Later on, Xia et al. studied how the microstructure and anisotropy induced by the electrically induced cure can lead to GNPs/epoxy nanocomposites with superior electrical and mechanical properties relative to those that are oven cured [18]. Such electrically conductive uncured nanocomposites containing different GNP loadings were later successfully used as adhesives to repair CFRPs through Joule heat curing, showing similar lap shear strengths to those found for the oven repaired samples, evidencing the effectiveness of this approach as an OoA method for CFRP repair [19]. However, the main focus of this prior work was the evaluation of the static strength of the joints bonded with an epoxy adhesive containing GNPs as the

conductive element, and the fatigue properties of such bonded joints were not investigated, despite this property being crucial for most of the applications. In addition, the effect of other types of nanofillers as conductive elements on the performance of the repaired components was not explored either.

Fatigue refers to the ability of adhesive joints to withstand cyclic loads without failing, and it strongly depends on the joint's configuration and intrinsic properties of the adhesive. The incorporation of different types of nanoparticles into the adhesive has been widely used for the last few decades as an effective strategy to improve the toughness and fatigue resistance of composites and structural adhesives [20,21]. Due to their low density, dimensions in the nanoscale and outstanding mechanical properties, carbon nanoparticles are particularly attractive to be used as adhesive modifiers, since they can render considerable improvements on the mechanical properties of adhesively bonded CFRP joints at very low loadings. For example, Kang et al. [22] incorporated 2 wt.% loading of MWCNTs into an epoxy adhesive and found a decrease in the static lap shear strength; however, they found an increase in the fatigue life of composites' adhesively bonded lap shear joints due to the promotion of longer crack initiation and propagation times through a mechanism of crack deflection when they are added into the adhesive. More recently, improvements on the fatigue life of CFRP bonded joints using an epoxy adhesive filled with GNPs have also been reported, with crack deflection also suggested as the main mechanism [23]. The addition of carbon nanomaterials (CNTs and GNPs) to structural adhesives emerges, thus, as particularly attractive for the development of OoA CFRP repair methods, since they can provide the electrical conductivity required for an effective Joule heat curing, while also providing adhesively bonded joints with improved lap shear strengths and fatigue resistance. However, this duality offered by carbon nanoparticles acting simultaneously as a conductive and toughening component in structural adhesives has not been properly investigated yet.

Herein, the potential of electrically conductive GNPs/epoxy, MWCNTs/epoxy and hybrid GNPs-MWCNTs/epoxy mixtures as Joule-cured adhesives for adhesively bonded joints with improved mechanical performances is investigated. The microstructure (i.e., dispersion and arrangement of the nanoparticles in the matrix) of the conductive nanocomposites with different formulations is evaluated and related to the distribution of the Joule heat generated upon the application of an electric field through them during the CFRP repair process, as well as to the mechanical properties of the repaired samples. The mechanical performance of the Joule-bonded CFRP joints is analyzed by static lap shear and fatigue tests and compared with that found for the joints bonded with neat epoxy as well as with their in-the-oven-bonded analogues to assess their potential as adhesives for Joule CFRP repair. Their failure mechanism is investigated by SEM to gain insight into and, thus, gain control of the formulation of conductive adhesives that can render an effective Joule bonding of CFRP joints with competitive lap shear strengths and fatigue resistances. The effect of the dimensionality of the carbon nanoparticles embedded into the epoxy adhesive on the electrical and Joule heating properties of the nanocomposites and, thus, on their Joule CFRP repair effectiveness and mechanical performance of the bonded joints is evaluated in order to gain control on the adhesive's formulation that will lead to optimization of the repair process.

2. Materials and Methods

2.1. Materials

Graphene nanoplatelets (GNPs) M25 from XG Science (East Lansing, MI, USA) with lateral dimensions $\sim 7.7 \mu\text{m}$ and thickness $\sim 6\text{--}8 \text{ nm}$, according to previous data reported in our group [24], and multi-walled carbon nanotubes (MWCNTs) Nanocyl TM NC7000 from Nanocyl S.A. (Sambreville, Belgium) with diameters and average lengths of $\sim 10 \text{ nm}$ and of $\sim 1.5 \mu\text{m}$, respectively, as quoted by the manufacturer, were used as nanofillers. The epoxy resin (Araldite, LY5052) and the hardener (Aradur, HY5052) were purchased from

Huntsman (The Woodlands, TX, USA), and 3K Hexcel HexTow[®] carbon fiber plain weave cloth with a grammage of 199 g/m² was purchased from Sigmalex (Runcorn, UK).

2.2. Fabrication and Characterization of Oven Cured Epoxy Nanocomposites

GNPs/epoxy and MWCNTs/epoxy nanocomposite mixtures with filler loadings in the range of 0–9 wt.% and 0–1 wt.%, respectively, were prepared following the experimental procedure reported in our previous work [19]. The nanocomposite mixtures were then oven-cured using the protocol recommended by the manufacturer, which comprises two steps: a pre-curing step where the mixture is left at room temperature for 24 h, followed by the curing step in which the material is heated in an oven at 100 °C for 4 h. A GNPs-MWCNTs/epoxy hybrid nanocomposite with 0.5 wt.% total nanofiller loading (GNPs:MWCNTs = 2:3) was also fabricated using the same experimental method.

The impedance of 15 × 15 × 0.5 mm nanocomposite specimens was measured through thickness using a Newtons4th Ltd. PSM 1735 Frequency Response Analyzer (Leicester, UK) connected with an Impedance Analysis Interface (IAI) in the range of frequencies 1–10⁶ Hz for all the formulations prepared. The specific conductivity of the samples was then calculated from the experimentally determined impedances using Equation (1):

$$\sigma(\omega) = |Y^*(\omega)| \frac{t}{A} = \frac{1}{Z^*} \times \frac{t}{A} \quad (1)$$

where $Y^*(\omega)$ is the complex admittance, Z^* is the complex impedance, and t and A are the thickness and cross-section area of the specimen, respectively.

The cryo-fracture of the epoxy and the nanocomposites was characterized by scanning electron microscopy (SEM) using a TescanSC Mira 3 microscope (Brno, Czechia) at an accelerating voltage of 5 kV.

2.3. CFRPs Repair through Adhesively Bonded Joints

Epoxy nanocomposite uncured mixtures containing 3 wt.% loading of GNPs, 0.5 wt.% loading of MWCNTs and a combination of both nanofillers with a total loading of 0.5 wt.% (GNPs:MWCNTs = 2:3) prepared following the method described in Section 2.2 were used as adhesives to repair CFRPs both in the oven and OoA. For the oven-based CFRP repair, the adhesives were spread onto the pre-treated adherend's bonding area, and the joint was assembled and cured following the oven curing cycle described in Section 2.2. (The fabrication of the CFRPs used as adherends and the surface modification of the bonding areas are described in Supplementary Materials). A uniform and controlled pressure was applied to the bonding area by placing a metal block on the joint in order to keep a constant adhesive layer thickness of ~0.2 mm. Control samples were repaired using neat epoxy as adhesive. For the Joule repair, the conductive mixtures were homogeneously spread onto the bonding area and two pieces of copper tape were attached at both sides of the joints to be used as electrodes, as schematically represented in Figure 1. (It should be noted that the electrodes are attached at both sides of the joints in order to avoid passing the electric current through the adherends. This set-up will ensure that only the adhesive is Joule-heated during the curing/repair process, providing highly localized heating and avoiding heating the adherends unnecessarily, which might lead to undesired structural damages on them, particularly if the T_g of the adherend is not much higher than the curing temperature of the adhesive). After the pre-curing step, a direct electric current of 5 V was applied through the adhesive along the out-of-plane direction using a DC power supply (Gw Instek, PSP-405, New Taipei, Taiwan). The generated Joule heat was monitored using an infrared (IR) camera (FLIR Q60, Wilsonville, OR, USA), and the applied voltage was carefully controlled to keep the temperature ~100 °C for 4 h to simulate the conditions used for the oven-repaired samples. An infrared camera detects the infrared energy of the tested material and transforms the acquired infrared data into an electronic image (thermograph) that shows its surface temperature. To ensure precise temperature measurements, the camera was calibrated by testing the temperature of boiling water, as recommended by the

manufacturer, showing a deviation of a few tenths of a degree Celsius. A constant voltage of ~5 V and a total power below 10 W were carefully kept during the Joule heat experiments in order to avoid overheating the material, since this would affect negatively the quality of the Joule-cured bonds. The heating rates were determined from the applied voltage.

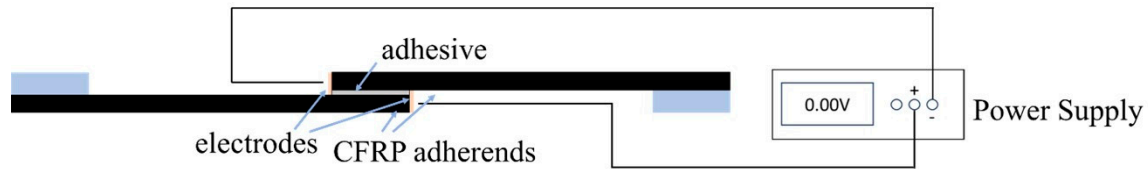


Figure 1. Schematic of the OoA CFRPs repair approach via Joule heat curing of electrically conductive epoxy nanocomposites.

The ultimate static strength of all the repaired CFRPs was evaluated by single-lap shear testing using an Instron 3365 machine following the standard ASTM D1002–10 (2019) with a load cell of 10 kN and a crosshead displacement rate of 1.3 mm/min. Two 25.4 × 25.4 mm CFRFs tabs were placed on both ends of the adherends to correct the alignment and eliminate the effect of eccentricity during the test. In order to evaluate the repeatability of the test, five specimens per sample were tested. Fatigue tests were performed on all the samples repaired using an Instron 8802 machine (Wycombe, UK) equipped with a 100 kN load cell, using sinusoidal waveforms at a stress ratio (R) of 0.1 and a frequency of 25 Hz. The stress level was varied from 0.9 to 0.5 and at least three specimens per sample were tested. The fracture surface of the samples was characterized by SEM, using a Tescan SC Mira 3 at an accelerating voltage of 5 kV to investigate the failure mechanism.

3. Results and Discussion

3.1. Electrical Conductivity of the Epoxy Nanocomposites

For an effective CFRP repair through adhesively bonded joints based on Joule heating, the adhesives need to be electrically conductive. It is, thus, essential to create an electrically conductive network of nanoparticles in the epoxy adhesive capable of generating enough heat through a Joule heating effect when an electric current is passed through them. The through-thickness electrical properties of ~500 μm thick specimens of the nanocomposites filled with GNPs and MWCNTs were evaluated, given that this will be the thickness of a typical bondline in the later mechanical testing. The variation in the through-thickness (i.e., out-of-plane) specific conductivity of 15 × 15 × 0.5 mm nanocomposites based on GNPs and MWCNTs with increasing filler loading is shown in Figure 2. Both systems behaved as electrically percolated systems, showing very low conductivities at low filler loadings and a rapid increase in conductivity with filler loadings above their percolation thresholds. The percolation threshold of each of these systems can be calculated using the classic percolation theory (Equation (2)), which assumes the filler particles are randomly distributed within the polymer matrix [25,26]:

$$\sigma = \sigma_0 (P - P_c)^t \quad (2)$$

where σ is the specific electrical conductivity, σ_0 is the fitted constant, P and P_c are the filler loading and the percolation threshold, respectively, and t is the conductivity exponent, which is related to the dimensionality of the conductive system.

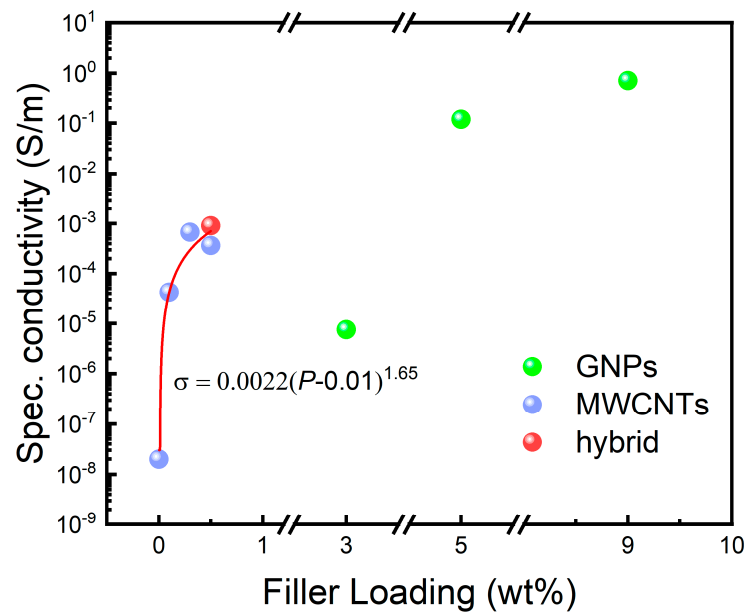


Figure 2. Variation in the out-of-plane specific electrical conductivity of $15 \times 15 \times 0.5$ mm GNP/epoxy, MWCNT/epoxy and hybrid/epoxy (GNPs:MWCNTs = 3:2) nanocomposites.

Using the classic percolation theory, values of ~ 3 wt.% and ~ 0.01 wt.% were found for the percolation thresholds of the systems based on GNPs and MWCNTs, respectively. The considerably lower percolation threshold found for the MWCNTs/epoxy nanocomposites relative to the GNP/epoxy ones was attributed to the higher aspect ratio of the 1D MWCNTs relative to the 2D graphene platelets [27], which is known to facilitate the formation of a conductive network of nanoparticles in the polymer matrix at lower loadings. Indeed, longer conductive nanoparticles can form conductive paths within the polymer matrix more easily by making contact with each other or through a tunnelling effect when they are close enough to each other; hence, lower amounts of longer nanoparticles are necessary to provide an insulating polymer matrix with electrical conductivity. A value of t of ~ 1.63 was found for the system based on MWCNTs from the data plotted in Figure 2, and a value of ~ 2.41 was previously found for the GNP-based system [19], suggesting that a 3D network of conductive particles is developed in the matrix above percolation in both cases, independently of the filler [19,28]. The higher t found for the MWCNTs system relative to the GNPs one suggests that the network of electrically conductive nanoparticles in the matrix develops faster with increasing filler loadings of MWCNTs above percolation due to the higher aspect ratio of the carbon nanotubes relative to the GNP flakes, which will also lead to high specific conductivities at lower loadings relative to the system based on GNPs. It should be highlighted that the maximum conductivities that these nanocomposites can achieve strongly depend on the intrinsic conductivity of each nanofiller. In this work, the specific conductivity for the MWCNTs/epoxy nanocomposite with a filler content of 0.3 wt.% ($\sim 10^{-3}$ S/m) was found to be two orders of magnitude higher than that obtained for the GNP/epoxy nanocomposite with a loading of 3 wt.% ($\sim 10^{-5}$ S/m).

In order to have electrically conductive nanocomposites with the minimum possible filler loading to avoid processing issues and ensure a good dispersion of the nanofiller particles in the matrix, the nanocomposites loaded with 3 wt.% GNPs and 0.5 wt.% MWCNTs (named as 3GNPs/epoxy and 0.5MWCNTs/epoxy, respectively) were selected to evaluate their Joule heating properties and their potential as Joule-cured adhesives for CFRP repair. (It should be noted that in the case of the GNPs system, a loading close to the percolation threshold was selected to avoid the large increments in viscosity and the formation of agglomerates typically observed at very high filler loadings). In addition to these two binary electrically conductive nanocomposites and taking advantage of the synergistic effect previously found when nanoparticles with different dimensionalities are

combined [18,29], a hybrid nanocomposite with a total filler loading of 0.5 wt.% and a GNPs–MWCNTs ratio of 2:3 was also fabricated. This hybrid nanocomposite containing 0.2 wt.% GNPs and 0.3 wt.% MWCNTs showed an electrical conductivity of 10^{-3} S/m (Figure 2), which was higher than the conductivities found for the two selected binary nanocomposites without having to add further filler, clearly showing the advantage of the hybrid system (i.e., ternary system) over the binary systems, thus also showing promise as an adhesive for Joule CFRPs repair.

3.2. Microstructure of the Epoxy Nanocomposites

Obtaining insight on the arrangement and level of dispersion of the nanoparticles in the matrix above their percolation thresholds is key to understanding the Joule heating properties of the adhesives as well as the mechanical performance of the repaired samples. Thus, the cryo-fracture surfaces of the epoxy and the three electrically conductive nanocomposites selected were characterized by SEM to evaluate their overall microstructure and assess the level of dispersion of the nanofiller particles in the epoxy matrix. Representative SEM images (Figure 3) show an absence of voids and structural defects in all the cases, suggesting that optimal conditions have been employed for the synthesis and processing of all the samples. A very smooth cryo-fracture surface was found for the neat epoxy (Figure 3a), whereas rougher surfaces were found for the nanocomposites (Figure 3b–d) due to the presence of the filler nanoparticles, with the GNP-based nanocomposite showing the roughest surface amongst all the nanocomposites under study, probably due to the higher filler loading that needs to be embedded into the matrix to make the GNPs/epoxy nanocomposite conductive relative to the other two, as discussed in Section 3.1.

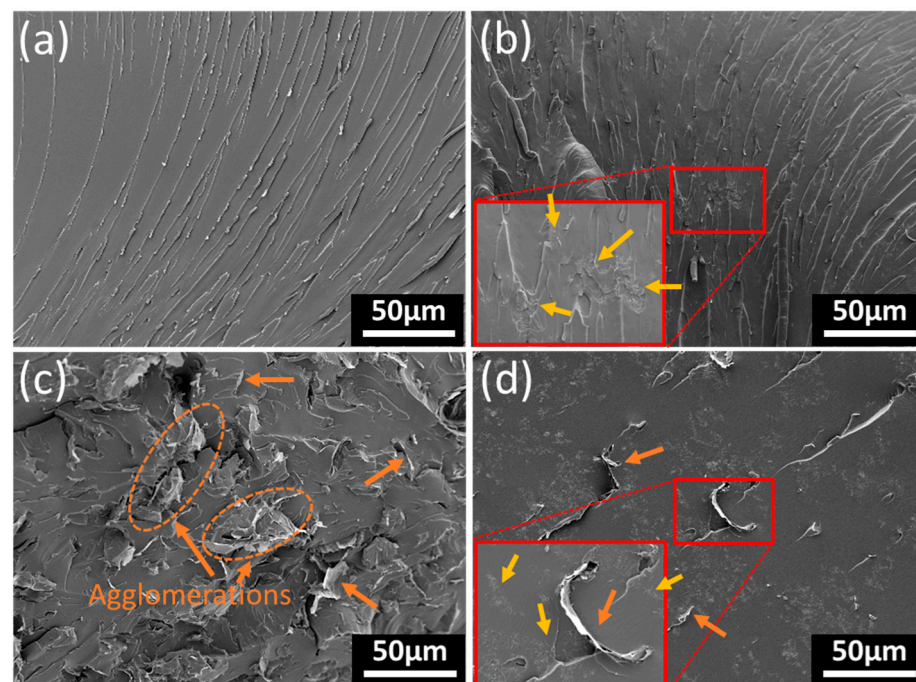


Figure 3. SEM images of the cryo-fractured surfaces of neat epoxy (a), and the 0.5MWCNTs (b), 3GNPs (c) and hybrid (d) nanocomposites. (The yellow arrows show the CNT agglomerates, and the orange arrows show the GNPs flakes and its agglomerates).

SEM images of the 0.5MWCNTs nanocomposite (Figure 3b) show the presence of some agglomerates of nanotubes in the epoxy matrix, which is attributed to the high aspect ratio and strong van der Waals forces and π - π interactions existing between individual MWCNTs, which makes their disentanglement into individually dispersed tubes very challenging. The presence of MWCNTs and small agglomerates of them could be, thus, easily found in the epoxy matrix even at this low filler loading (0.5 wt.%), with them

being, however, uniformly distributed all throughout the matrix. In the case of the 3GNPs nanocomposite (Figure 3c), the graphene flakes were generally well distributed within the matrix, with a few small agglomerates being found. Overall, the hybrid nanocomposite (Figure 3d) showed a better distribution of the GNPs and MWCNTs relative to the binary nanocomposites, which may be due to the lower loadings of both nanofillers incorporated in this hybrid system. In addition, some GNP flakes in the hybrid nanocomposite were found to act as bridges connecting small agglomerates of MWCNTs, with the higher conductivity found for the hybrid nanocomposite relative to the two binary systems being attributed to this arrangement of filler particles.

3.3. CFRPs Repair by Joule Heat Curing of the Conductive Epoxy Nanocomposites

The 3GNPs, 0.5MWCNTs and the hybrid nanocomposites were used as Joule-cured adhesives for CFRP repair. In a typical repair process, the conductive epoxy/nanofiller uncured mixtures were homogeneously spread on the bonding area between two laminates of CFRPs, as described in Section 2.3, and a direct electric current was passed through the adhesive along the out-of-plane direction. In order to mimic the oven curing conditions recommended by the manufacturer, the applied voltage was carefully controlled to reach 100 °C and hold the temperature for 4 h.

The distribution of the Joule heat generated during curing was obtained using an IR camera, and the obtained results are shown in Figure 4. It can be seen that when an electric current is applied through the adhesive mixtures (Figure 4d,e), two thermal peaks were identified in the bonding area, at 96 °C and 104 °C for the GNPs mixture, and at 99 °C and 111 °C for the MWCNTs mixture, which are assumed to be related to the dispersion of the nanofiller in the matrix. As discussed above, SEM revealed the presence of some small agglomerates of nanoparticles in both the GNP- and the MWCNT-based nanocomposites, resulting in some regions having a lower density of tubes/flakes than others, and hence leading to an inhomogeneous distribution of the generated Joule heat in the bonding area [15]. Furthermore, the fact that the two thermal peaks seen for the GNP-based nanocomposite are quite close to each other and show similar intensities, whereas for the MWCNT-based system, the two thermal peaks are more separated from each other and show considerably different intensities, suggests that the GNP system renders a more densely packed conductive network, relative to the MWCNT system, which contains a lower loading of filler particles.

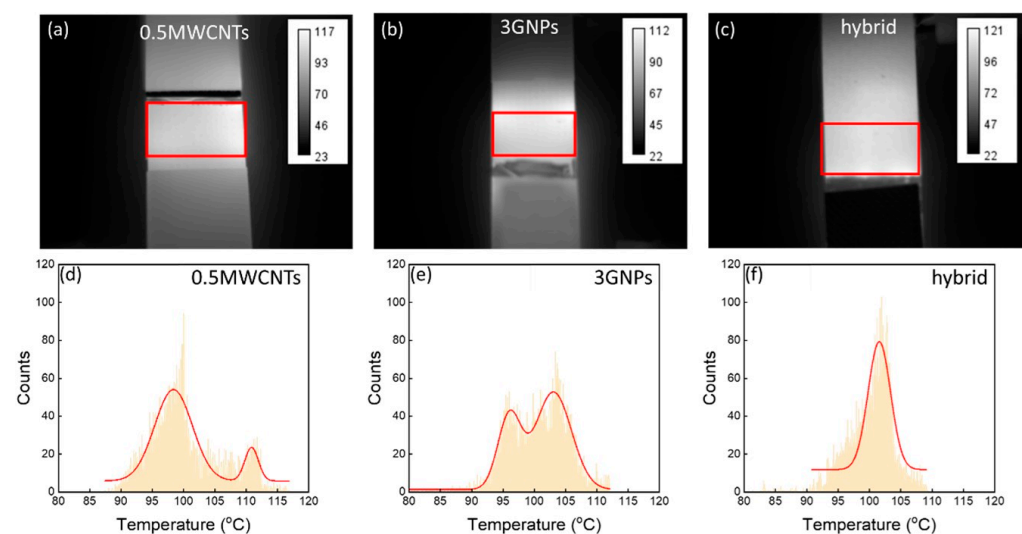


Figure 4. IR-camera images (a–c) and distribution of the generated Joule heat within the bonding area (d–f) for the 3GNPs, 0.5MWCNTs and hybrid nanocomposite mixtures during a typical OoA CFRPs repair.

For the hybrid system, however, a single thermal peak at ~ 107 °C was observed (Figure 4f), suggesting a more homogeneous distribution of the generated Joule heat all over the bonding area. This behavior may be attributed to the better dispersion found for the hybrid system relative to the two binary systems, discussed in Section 3.1. The addition of a relatively low amount of GNP flakes (0.2 wt.%) onto an adhesive containing 0.3 wt.% loading of MWCNTs seems to enhance the overall distribution of the generated Joule heat within the bonding area, with some of the flakes acting as bridges between the MWCNTs or their small agglomerates, thus leading to a more uniform conductive network of nanoparticles in the epoxy matrix and a more homogeneous distribution of the generated Joule heat. This better dispersion would also explain the higher specific conductivity found for the hybrid system.

3.4. Mechanical Properties of the Adhesively Bonded Single Lap Joints

The static and dynamic strength of the CFRP joints were evaluated by single-lap shear and fatigue tests, respectively, and compared with those obtained when neat epoxy and the nanocomposites were used as adhesives and oven cured.

3.4.1. Lap Shear Tests

The lap shear stress–strain curves obtained for the single-lap shear joints adhesively bonded by neat epoxy and the nanocomposites show the typical behavior of brittle materials without a plastic deformation zone, with such behavior being very similar in all the cases (Figure 5a). As shown in Figure 5b, the lap shear strength (LSS) obtained for the joints repaired using the nanocomposites as adhesives (~ 13 – 14 MPa) was very close to the LSS value found for the sample repaired using neat epoxy, independently of the nanocomposite's formulation. It should be highlighted that, even though higher values for the LSS of the systems based on GNPs would have been expected a priori relative to those found for the MWCNT-based one, due to their 2D nature typically providing higher shear and tensile strengths, the obtained values were very close to those found for the MWCNTs based system. We attribute this observation to the higher GNP loading required to be incorporated into the epoxy matrix relative to the MWCNTs to make the nanocomposite electrically conductive (a considerably higher percolation threshold was found for the GNP nanocomposite relative to the MWCNT-based one, as discussed in Section 3.1). The higher GNP loading incorporated into the epoxy matrix (3 wt.%) must, thus, lead to the formation of more agglomerates, impeding the achievement of its maximum potential as reinforcement, hence showing LSS values which are very close to those found for the adhesive filled with a considerably lower loading of MWCNTs (0.5 wt.%). No effect of the curing method employed to bond the joints on the LSS could be found either, obtaining very similar performances for the Joule-cured samples and the samples cured in the oven.

3.4.2. Fatigue Tests

The dynamic strength of all the specimens prepared was also tested to evaluate the fatigue properties of the bonded joints. As shown in Figure 6a, when the stress level applied to the sample during the fatigue tests (defined here as the maximum applied stress, σ_{max} , relative to the ultimate strength, σ_{ult} , obtained from the static single lap shear tests) was decreased from 0.9 to 0.5, the lifetime of all the adhesively bonded joints was found to increase linearly by several orders of magnitude, reaching the 'unbreakable' status (defined as not failing after 10^7 cycles) under a stress level below 0.5. These prolonged lives observed for all the joints under progressively lower stress levels must be attributed to a reduction in the crack initiation and propagation rates within the adhesives when lower stress levels, that is when milder conditions, are applied to the samples [30].

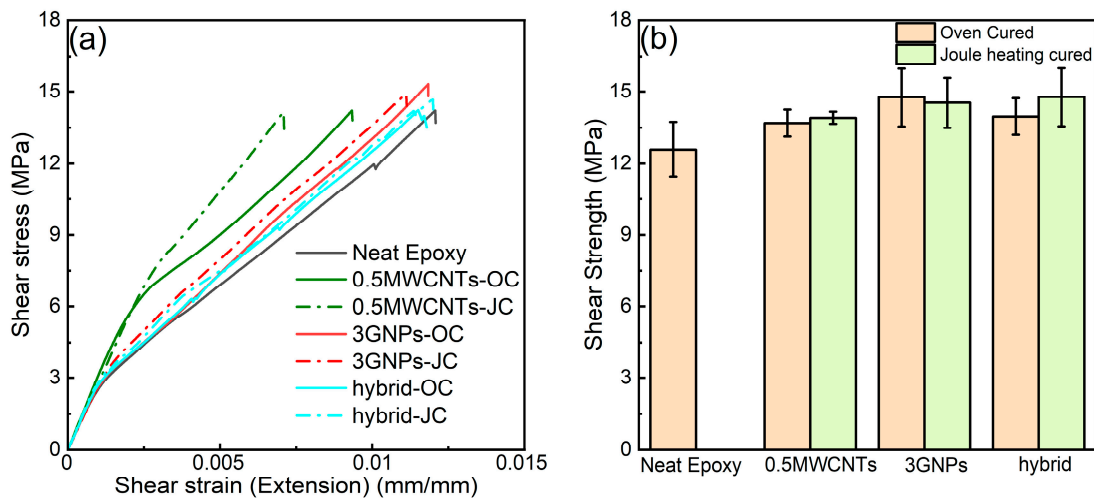


Figure 5. Stress–strain curves from single-lap shear tests (a) and LSS (b) of the CFRPs joints bonded using neat epoxy and the 3GNPs, 0.5MWCNTs and hybrid oven-cured (OC) and Joule-heat-cured (JC) nanocomposites.

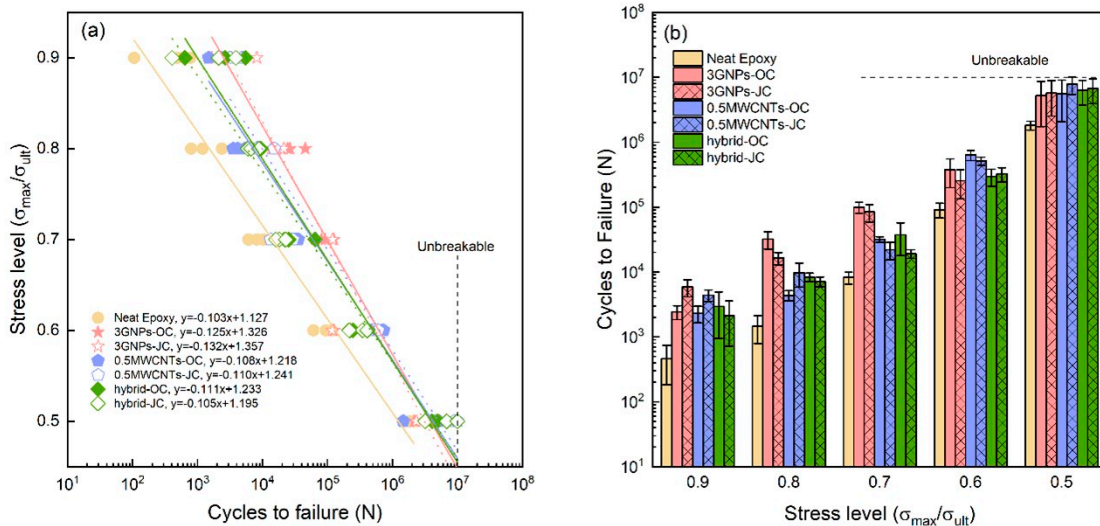


Figure 6. (a) S–N curves showing the relationship between the applied stress levels and number of cycles to failure for the adhesively bonded single-lap joints bonded with neat epoxy and the oven-cured (OC) and Joule-heat-cured (JC) nanocomposites, (b) bar chart of the average fatigue life and deviation.

Figure 6b shows the average cycles to failure found for the different samples tested and their respective deviations across the various stress levels studied. It can be seen that the joints adhesively bonded with the nanocomposites showed an enhanced fatigue life relative to those bonded with neat epoxy. In adhesively bonded joints, crack initiation is known to primarily occur at the end of the bonded area or at the interface between adhesive and adherend as a result of stress concentration. Once initiated, those cracks start to propagate through the adhesive, leading eventually to the sample’s failure. When a propagating crack encounters an obstacle, e.g., a nanoparticle, the crack is, in general, believed to be deflected around it, resulting in a longer crack propagation path, thereby contributing to an improvement in the fatigue life of the bonded joints [14,29]. This interaction between propagating cracks and nanoparticles effectively retards the progression of the cracks and has been widely accepted as the failure mechanism in similar nanocomposite systems [31,32]. More specifically, the incorporation of CNTs and GNPs into epoxy resins has been previously reported to effectively increase their toughness at relatively low

loadings through slightly different mechanisms [33]. In the case of adding CNTs, the epoxy toughening is believed to be due to their highly flexible elastic performance under both tensile and compressive loading, with individual nanotubes sliding within the bundles, with crack-bridging being accepted as the main toughening mechanism. The incorporation of GNPs was also found to improve the toughness of neat epoxy, also confirming graphene materials as an effective toughener for epoxies, with crack deflection being suggested as the major graphene toughening mechanism in this case. Furthermore, this enhanced fatigue behavior observed when the nanocomposites are used as adhesives, relative to when neat epoxy was used, was found to be increasingly pronounced under higher stress levels, as revealed by the higher slopes found from the linear fittings in Figure 6a. Such increasingly harsh conditions may promote the formation of a higher number of cracks within the adhesive relative to when lower stresses are applied; hence, the difference between the crack propagation paths in the nanocomposites relative to the neat epoxy will be increasingly more pronounced. The addition of nanoparticles to the epoxy adhesive seems, thus, to have an effect on prolonging the samples' life under all the stress levels studied, with this effect being increasingly pronounced as the test conditions become harsher.

Amongst the three nanocomposites studied here, the fatigue life of the lap joints bonded with the 3GNPs one was found to be slightly superior under stress levels ≥ 0.7 than those observed for both the 0.5MWCNTs and the hybrid nanocomposites (Figure 6b), suggesting that 2D nanoparticles must lead to a more effective crack deflection and energy absorption than 1D nanoparticles, in agreement with previous reports [34]. This observation can be attributed to the 2D nanoparticles providing larger contact areas between the filler particles and the epoxy, allowing them to absorb more energy during the sample's deformation relative to when just 1D MWCNTs or 1D MWCNTs combined with a low content of 2D GNPs are incorporated into the adhesive, eventually leading to a more effective crack deflection and, hence, to a longer fatigue life. In addition, it should be mentioned that the nanocomposite based on GNPs contained higher filler loading (3 wt.%) than the other two (0.5 wt.%), due to its higher percolation threshold, which must also contribute to these more effective crack deflections and longer fatigue lives observed. At lower stress levels (<0.7), however, similar results were found for all the samples, independently of their formulation, with their fatigue lives being found to converge (Figure 6a). This suggests that the adhesives containing MWCNTs (both the one purely based on MWCNTs and the hybrid) render similar mechanical performances to those found for the adhesive based on GNPs when low stress levels are applied. Finally, like for the lap shear results, similar fatigue performances were also found independently of the curing method employed, which suggests that the Joule cure and the oven-based CFRP repair methods seem to be equally effective.

3.4.3. Failure Mechanism of the Adhesively Bonded Joints

In order to gain control on the failure of the joints adhesively bonded using neat epoxy and the nanocomposites, it is important to investigate their failure mechanism. The failure modes typically observed in adhesively bonded joints include adhesive or interfacial, cohesive, and light-fiber tear failure, as schematically represented in Supplementary Materials, with a combination of different mechanisms being the most common situation.

SEM analysis was performed on the fracture surface of the joints bonded with neat epoxy and the nanocomposites after fatigue tests performed under different stress levels from 0.5 to 1 in order to investigate their failure mechanisms, and representative images are shown in Figure 7. When neat epoxy was used as the adhesive (Figure 7a), the presence of fiber tracks, textured microflow and cusps observed on the fracture surface of the sample, combined with small regions covered by debris from the adhesive, suggests the coexistence of both adhesive and cohesive failure mechanisms, with the adhesive dominating the system's failure over the cohesive [35–37]. The fracture surface of the nanocomposites tested under identical conditions (Figure 7b–g) showed similar features to those found for the samples bonded with neat epoxy, with both the cohesive and the adhesive failure

mechanisms coexisting. However, in these cases, the SEM images reveal the presence of more extensive regions covered by debris from the nanocomposites used as adhesives, suggesting an increased contribution of the cohesive mechanism relative to the adhesive. This observation indicates an enhanced interface between the nanocomposite adhesive and the CFRP adherends relative to the interface between neat epoxy and adherend, with similar results found independently of the stress level applied to the samples during the fatigue test (shown in Supplementary Materials). Furthermore, no clear effect of the specific type of nanofiller incorporated into the adhesive or the method employed to cure it on the failure mechanism could be found.

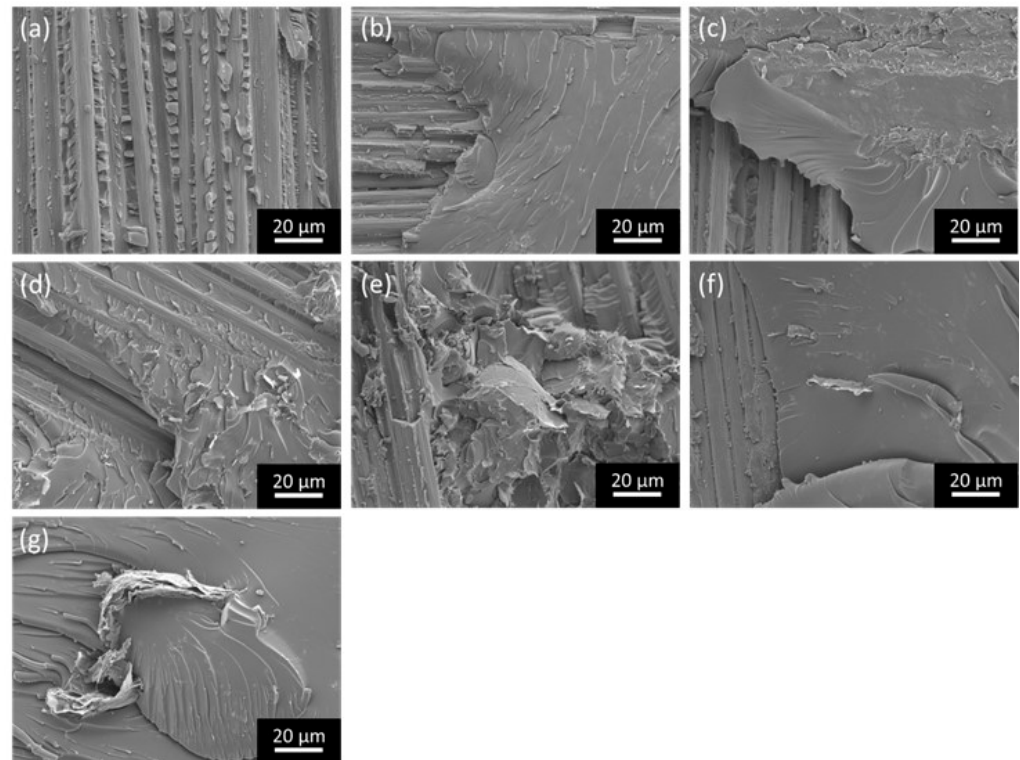


Figure 7. SEM images of the fracture surface of the joints bonded with neat epoxy (a), 0.5MWCNTs-OC (b), 0.5MWCNTs-JC (c), 3GNPs-OC (d), 3GNPs-JC (e), hybrid-OC (f) and hybrid-JC (g), after fatigue tests performed at a stress level of 0.9.

In summary, the three conductive nanocomposites studied as adhesives have been proved to be effective in leading to successful CFRP repair through Joule heat curing, with the bonded joints showing LSSs which are comparable to those found when neat epoxy is used as an adhesive and oven cured, and improved fatigue resistance promoted through a mechanism of crack deflection. No clear effect of the nanocomposite's formulation was found though, suggesting that a well-distributed conductive network of any type of carbon nanoparticles must lead to a successful Joule repair with bonded joints with good performance. However, the incorporation of MWCNTs vs. GNPs into the adhesive has been found to considerably reduce the adhesive filler loading required for a successful repair, due to their much lower percolation threshold. The stronger adhesive–adherend interfaces promoted by adding nanofillers to the adhesive suggest, however, that in order to further improve the mechanical performance of the bonded joints, strategies to enhance the adhesives toughness need now to be developed.

4. Conclusions

The potential of electrically conductive GNPs/epoxy, MWCNTs/epoxy and GNPs-MWCNTs/epoxy hybrid nanocomposite mixtures as adhesives for OoA and in-the-field CFRPs repair via Joule heating of the conductive network of carbon nanoparticles embed-

ded in the epoxy matrix was investigated. Above percolation, the three nanocomposites showed a good distribution of their conductive networks in the epoxy matrix, which led to a successful Joule thermoset curing and, hence, to a successful CFRP repair. The joints adhesively bonded with neat epoxy and the nanocomposites (both in the oven- and Joule-cured) showed similar lap shear strengths in all the cases, whereas the presence of nanoparticles in the adhesive was found to enhance the fatigue performance of the bonded joints relative to when neat epoxy was used as an adhesive, probably through a mechanism of crack deflection. Similar results were found independently of the adhesive's formulation, which suggests that the incorporation of MWCNTs as the only or one of the conductive components into the adhesive can considerably reduce the filler loading required for successful Joule repair, due to the lower percolation thresholds typically found for the hybrid and the MWCNTs/epoxy nanocomposite relative to the one based on GNPs and reaching similar mechanical performances. The fracture surface of the joints bonded with the three nanocomposites showed similar features to those found for the samples bonded using neat epoxy, with both cohesive and adhesive failure mechanisms coexisting, however, with more contribution of the cohesive relative to the adhesive, suggesting stronger adhesive–adherend interactions. Similar results were obtained independently of the curing method, evidencing the promise of this thermosets curing strategy based on Joule heating of conductive nanocomposites as an OoA and in-the-field method for CFRP repair with improved fatigue resistance relative to when neat epoxy is used as an adhesive and oven-cured, and with similar lap shear strengths. Strategies to improve their toughness should now be developed to improve the overall performance of the repaired CFRPs and make them suitable for highly demanding applications.

Supplementary Materials: The following supporting information can be downloaded at: <https://www.mdpi.com/article/10.3390/jcs8030112/s1>, Section S1. Fabrication and surface modification of the CFRP laminates (adherends); Figure S1: Schematic of the typical failure mechanisms occurring in adhesively bonded joints: (a) adhesive failure, (b) cohesive failure, (c) light-fiber-tear failure and (d) a mixed failure type; Figure S2: SEM images of the fracture surface of the lap shear joints bonded by different types of adhesives after fatigue test with the stress level of 0.9, 0.7, 0.6, and 0.5.

Author Contributions: Conceptualization, Y.H., I.A.K. and C.V.; methodology, Y.H.; validation, Y.H.; formal analysis, Y.H.; investigation, Y.H., I.A.K. and C.V.; data curation, Y.H.; writing—original draft preparation, Y.H.; writing—review and editing, Y.H., I.A.K. and C.V.; supervision, C.V.; funding acquisition, I.A.K. and C.V. All authors have read and agreed to the published version of the manuscript.

Funding: The authors would like to acknowledge the European Union's Horizon 2020 research and innovation program EU-Horizon 2020 RIA ("Graphene Core 3" GA: 881603) and the Henry Royce Institute for Advanced Materials, funded by EPSRC grants EP/R00661X/1, EP/S019367/1, EP/P025021/1 and EP/P025498/1 for funding this work. Ian A. Kinloch also acknowledges the Royal Academy of Engineering (RCSRF1819\7\30) and Morgan Advanced Materials for funding his chair, and Yuheng Huang would like to acknowledge the Graphene NOWNANO CDT for funding his PhD.

Data Availability Statement: Data are contained within the article and Supplementary Materials.

Conflicts of Interest: The authors declare no conflicts of interest. The funders had no role in the design of the study; in the collection, analyses, or interpretation of data; in the writing of the manuscript; or in the decision to publish the results.

References

1. Meng, F.; Olivetti, E.A.; Zhao, Y.; Chang, J.C.; Pickering, S.J.; McKechnie, J. Comparing Life Cycle Energy and Global Warming Potential of Carbon Fiber Composite Recycling Technologies and Waste Management Options. *ACS Sustain. Chem. Eng.* **2018**, *6*, 9854–9865. [[CrossRef](#)]
2. Industry ARC. Composite Materials Market—Forecast (2024–2030). Available online: <https://www.industryarc.com/Report/246/composite-materials-market-analysis-report.html> (accessed on 18 January 2024).

3. Amilhat, J. Fly the Green Deal, Europe's Vision for Sustainable Aviation, Report of the Advisory Council for Aviation Research and Innovation in Europe (ACARE). Available online: https://www.acare4europe.org/wp-content/uploads/2022/06/20220815_Fly-the-green-deal_LR-1.pdf (accessed on 4 March 2024).
4. Tsai, W.-H.; Chang, Y.-C.; Lin, S.-J.; Chen, H.-C.; Chu, P.-Y. A Green Approach to the Weight Reduction of Aircraft Cabins. *J. Air Transp. Manag.* **2014**, *40*, 65–77. [[CrossRef](#)]
5. Zhang, J.; Chevali, V.S.; Wang, H.; Wang, C.-H. Current Status of Carbon Fibre and Carbon Fibre Composites Recycling. *Compos. Part B Eng.* **2020**, *193*, 108053. [[CrossRef](#)]
6. McConnell, V.P. Launching the Carbon Fibre Recycling Industry. *Reinf. Plast.* **2010**, *54*, 33–37. [[CrossRef](#)]
7. Rademacker, T. *Challenges in CFRP Recycling*; Federal Ministry for Economic Affairs and Energy: Berlin, Germany, 2018; pp. 24–25.
8. Vinson, J.R. Mechanical Fastening of Polymer Composites. *Polym. Eng. Sci.* **1989**, *29*, 1332–1339. [[CrossRef](#)]
9. Banea, M.D.; da Silva, L.F.M. Adhesively Bonded Joints in Composite Materials: An Overview. *Proc. Inst. Mech. Eng. Part L J. Mater. Des. Appl.* **2009**, *223*, 1–18. [[CrossRef](#)]
10. Kinloch, A.J.; Lee, J.H.; Taylor, A.C.; Sprenger, S.; Eger, C.; Egan, D. Toughening Structural Adhesives via Nano- and Micro-Phase Inclusions. *J. Adhes.* **2003**, *79*, 867–873. [[CrossRef](#)]
11. Saba, N.; Jawaid, M.; Allothman, O.Y.; Paridah, M.; Hassan, A. Recent Advances in Epoxy Resin, Natural Fiber-Reinforced Epoxy Composites and Their Applications. *J. Reinf. Plast. Compos.* **2016**, *35*, 447–470. [[CrossRef](#)]
12. Ahmadi, Z. Nanostructured Epoxy Adhesives: A Review. *Prog. Org. Coat.* **2019**, *135*, 449–453. [[CrossRef](#)]
13. Centea, T.; Grunenfelder, L.K.; Nutt, S.R. A Review of Out-of-Autoclave Prepregs—Material Properties, Process Phenomena, and Manufacturing Considerations. *Compos. Part A Appl. Sci. Manuf.* **2015**, *70*, 132–154. [[CrossRef](#)]
14. Kernin, A.; Wan, K.; Liu, Y.; Shi, X.; Kong, J.; Bilotti, E.; Peijs, T.; Zhang, H. The Effect of Graphene Network Formation on the Electrical, Mechanical, and Multifunctional Properties of Graphene/Epoxy Nanocomposites. *Compos. Sci. Technol.* **2019**, *169*, 224–231. [[CrossRef](#)]
15. Redondo, O.; Prolongo, S.G.; Campo, M.; Sbarufatti, C.; Giglio, M. Anti-Icing and de-Icing Coatings Based Joule's Heating of Graphene Nanoplatelets. *Compos. Sci. Technol.* **2018**, *164*, 65–73. [[CrossRef](#)]
16. Mas, B.; Fernández-Blázquez, J.P.; Duval, J.; Bunyan, H.; Vilatela, J.J. Thermoset Curing through Joule Heating of Nanocarbons for Composite Manufacture, Repair and Soldering. *Carbon* **2013**, *63*, 523–529. [[CrossRef](#)]
17. Prolongo, S.G.; Moriche, R.; Del Rosario, G.; Jiménez-Suárez, A.; Prolongo, M.G.; Ureña, A. Joule Effect Self-Heating of Epoxy Composites Reinforced with Graphitic Nanofillers. *J. Polym. Res.* **2016**, *23*, 189. [[CrossRef](#)]
18. Xia, T.; Zeng, D.; Li, Z.; Young, R.J.; Vallés, C.; Kinloch, I.A. Electrically Conductive GNP/Epoxy Composites for out-of-Autoclave Thermoset Curing through Joule Heating. *Compos. Sci. Technol.* **2018**, *164*, 304–312. [[CrossRef](#)]
19. Huang, Y.; Xia, T.; Kinloch, I.; Vallés, C. Graphene Nanoplatelets/Epoxy Nanocomposites as Conductive Adhesives for out-of-Autoclave in-Situ CFRPs Repair. *Compos. Sci. Technol.* **2023**, *237*, 110007. [[CrossRef](#)]
20. Marouf, B.T.; Mai, Y.-W.; Bagheri, R.; Pearson, R.A. Toughening of Epoxy Nanocomposites: Nano and Hybrid Effects. *Polym. Rev.* **2016**, *56*, 70–112. [[CrossRef](#)]
21. Kinloch, A.J. Toughening Epoxy Adhesives to Meet Today's Challenges. *MRS Bull.* **2003**, *28*, 445–448. [[CrossRef](#)]
22. Kang, M.-H.; Choi, J.-H.; Kweon, J.-H. Fatigue Life Evaluation and Crack Detection of the Adhesive Joint with Carbon Nanotubes. *Compos. Struct.* **2014**, *108*, 417–422. [[CrossRef](#)]
23. Sadigh, M.A.S.; Marami, G. Enhancing Fatigue Life in Adhesively Bonded Joints Using Reduced Graphene Oxide Additive: Experimental and Numerical Evaluation. *Int. J. Adhes. Adhes.* **2018**, *84*, 283–290. [[CrossRef](#)]
24. Young, R.J.; Liu, M.; Kinloch, I.A.; Li, S.; Zhao, X.; Vallés, C.; Papageorgiou, D.G. The Mechanics of Reinforcement of Polymers by Graphene Nanoplatelets. *Compos. Sci. Technol.* **2018**, *154*, 110–116. [[CrossRef](#)]
25. Last, B.J.; Thouless, D.J. Percolation Theory and Electrical Conductivity. *Phys. Rev. Lett.* **1971**, *27*, 1719–1721. [[CrossRef](#)]
26. Bauhofer, W.; Kovacs, J.Z. A Review and Analysis of Electrical Percolation in Carbon Nanotube Polymer Composites. *Compos. Sci. Technol.* **2009**, *69*, 1486–1498. [[CrossRef](#)]
27. Singh, N.P.; Gupta, V.K.; Singh, A.P. Graphene and Carbon Nanotube Reinforced Epoxy Nanocomposites: A Review. *Polymer* **2019**, *180*, 121724. [[CrossRef](#)]
28. Dong, M.; Zhang, H.; Tzounis, L.; Santagiuliana, G.; Bilotti, E.; Papageorgiou, D.G. Multifunctional Epoxy Nanocomposites Reinforced by Two-Dimensional Materials: A Review. *Carbon* **2021**, *185*, 57–81. [[CrossRef](#)]
29. Kyrlyuk, A.V.; Hermant, M.C.; Schilling, T.; Klumperman, B.; Koning, C.E.; van der Schoot, P. Controlling Electrical Percolation in Multicomponent Carbon Nanotube Dispersions. *Nat. Nanotechnol.* **2011**, *6*, 364–369. [[CrossRef](#)] [[PubMed](#)]
30. Mouritz, A. Fatigue of Aerospace Materials. In *Introduction to Aerospace Materials*; Elsevier: Amsterdam, The Netherlands, 2012; pp. 469–497. ISBN 978-1-85573-946-8.
31. Johnsen, B.B.; Kinloch, A.J.; Mohammed, R.D.; Taylor, A.C.; Sprenger, S. Toughening Mechanisms of Nanoparticle-Modified Epoxy Polymers. *Polymer* **2007**, *48*, 530–541. [[CrossRef](#)]
32. Parente, J.M.; Santos, P.; Valvez, S.; Silva, M.P.; Reis, P.N.B. Fatigue Behaviour of Graphene Composites: An Overview. *Procedia Struct. Integr.* **2020**, *25*, 282–293. [[CrossRef](#)]
33. Hsieh, T.H.; Kinloch, A.J.; Masania, K.; Taylor, A.C.; Sprenger, S. The Mechanisms and Mechanics of the Toughening of Epoxy Polymers Modified with Silica Nanoparticles. *Polymer* **2010**, *51*, 6284–6294. [[CrossRef](#)]

34. Knoll, J.B.; Riecken, B.T.; Kosmann, N.; Chandrasekaran, S.; Schulte, K.; Fiedler, B. The Effect of Carbon Nanoparticles on the Fatigue Performance of Carbon Fibre Reinforced Epoxy. *Compos. Part A Appl. Sci. Manuf.* **2014**, *67*, 233–240. [[CrossRef](#)]
35. Casas-Rodriguez, J.P.; Ashcroft, I.A.; Silberschmidt, V.V. Damage in Adhesively Bonded CFRP Joints: Sinusoidal and Impact-Fatigue. *Compos. Sci. Technol.* **2008**, *68*, 2663–2670. [[CrossRef](#)]
36. Pang, Y.-Y.; Wu, G.; Su, Z.-L.; He, X.-Y. Experimental Study on the Carbon-Fiber-Reinforced Polymer–Steel Interfaces Based on Carbon-Fiber-Reinforced Polymer Delamination Failures and Hybrid Failures. *Adv. Struct. Eng.* **2020**, *23*, 2247–2260. [[CrossRef](#)]
37. Rahman, N.M.; Sun, C.T. Strength Calculation of Composite Single Lap Joints with Fiber-Tear-Failure. *Compos. Part B Eng.* **2014**, *62*, 249–255. [[CrossRef](#)]

Disclaimer/Publisher’s Note: The statements, opinions and data contained in all publications are solely those of the individual author(s) and contributor(s) and not of MDPI and/or the editor(s). MDPI and/or the editor(s) disclaim responsibility for any injury to people or property resulting from any ideas, methods, instructions or products referred to in the content.